JOURNAL OF MATERIALS SCIENCE 28 (1993) 5056–5059

Observations on particle size/spacing relationships and phase equilibria in the Cu–Ni–Cr system

FEHIM FINDIK
Istanbul Technical University, Sakarya Engineering Faculty, 54188 Adapazari, Turkey

The development of increased strength in Cu–Ni–Cr alloys, compared to binary Cu–Ni alloys, depends upon heat treatment. Alloys have compositions which permit them to be solution treated at elevated temperature and then aged at a lower temperature, in a two-phase field, to produce hardening. The decomposition into two phases may occur by nucleation and growth or by a spinodal reaction, depending on the alloy composition and the heat-treatment temperature. In this study, the relationship between particle size and wavelength (interparticle spacing) was studied in some Cu–Ni–Cr spinodal alloys and it was found that the wavelength was directly proportional to the particle size. Also, the Cu–Ni–Cr ternary diagram at the 930 °C isothermal section was similar to that obtained by Meijering *et al.*

1. Introduction

The idea of a spinodal was formulated at the same time as nucleation theory, and both concepts were discussed by Gibbs [1] in 1877. The thermodynamic criterion for a spinodal is that the second derivative of the free energy, G, with respect to composition, C, is zero. Inside a spinodal, where $\partial^2 G/\partial C^2 < 0$, no activation barrier for nucleation exists as in a metastable solid solution, and consequently the unstable solid solution spontaneously decomposes. Hence, Gibbs referred to a spinodal as the limit of metastability. Spinodal decomposition is characterized by small composition fluctuations over large distances, whereas a classical nucleation process is characterized by large composition variations over small distances. Since the new phases form by a continuous diffusional process with a gradual change in composition across the interface, they must have similar crystal structures to the original solid solution and they are coherent. The resulting microstructure consists of a uniform dispersion of small, coherent interconnected particles. Experimental observations have shown that spinodal decomposition occurs in metallic, ceramic and glass systems.

The Cu–Ni binary system is considered to be an ideal isomorphous system. However, the addition of a ternary alloying element such as Fe, Sn or Cr is known to introduce miscibility gaps which make these alloys susceptible to heat treatment. Cu–Ni–Fe alloys are widely used as magnetic materials, Cu–Ni–Sn alloys, after appropriate heat treatment, possess very high elastic limits which make them attractive as for spring materials. Cu–Ni–Cr alloys find application as condenser tubes in marine atmospheres [2, 3].

A number of investigations have been carried out on the transformations in Cu–Ni–Cr alloys with compositions in the vicinity of the miscibility gap. The miscibility gap in the Cu–Ni–Cr system was first reported by Meijering *et al.* [4, 5] by means of metallographic and X-ray diffraction (XRD) methods, an isothermal section was determined at 930 °C. In this work, two face-centred-cubic phases rich in copper and nickel and one body-centred-cubic phase rich in chromium were found to exist, although the binary Cu–Ni alloys show complete miscibility. Investigations have been carried out on some Cu–Ni–Cr alloys in the composition range close to the copper-rich end of the miscibility gap with the primary aim of developing a substitute for the conventional 70Cu–30Ni alloy with higher strength, for applications in a marine atmosphere. These studies have led to considerable ambiguity regarding the nature of the decomposition in alloys in this region of the miscibility gap. In the present work, Cu–30Ni–2.5Cr, Cu–30Ni–5Cr, Cu–45Ni–10Cr and Cu–45Ni–15Cr (all wt %) alloys were investigated. These alloys have commercial importance due to their good weldability, a higher strength than the conventional Cu–30Ni alloy, and good corrosion resistance in marine atmospheres. The 10%Cr and 15%Cr alloys lie at the centre of the miscibility gap while the 2.5%Cr and 5%Cr alloys lie at the Cu-rich end of the miscibility gap. Previous work [2, 3] did not include the particle size/spacing relationship for similar alloys. In the present work, a particle size/spacing (p/λ) relationship is included and the phase equilibria in the Cu–Ni–Cr system is compared with the previous work [4, 5].

2. Experimental procedure

Alloys of nominal compositions Cu–30 wt % Ni–2.5 wt % Cr, Cu–30 wt % Ni–5 wt % Cr, Cu–45 wt % Ni–10 wt % Cr and Cu–45 wt % Ni–15 wt % Cr were prepared by melting pure copper (99.999%), nickel

0022–2461

(99.9%) and chromium (99.9%) in a vacuum arc furnace. Chemical analysis of the alloys by X-ray energy-dispersive (X-EDS) analysis showed the actual compositions.

After casting and checking the composition, cast buttons were cut to a 2 mm thickness and homogenized as defined in [6, 7]. Heat treatments were carried out in a vertical-tube furnace. The temperature within the hot zone of the furnace was controlled to an accuracy of $\pm 5\,^{\circ}C$. Ageing times from 5 min to 3 weeks were employed, and after ageing in the range 300–930 °C all specimens were fast quenched into iced water. Thin-foil preparation was done as in [6, 7] using a solution of 25% nitric acid in methanol .

The foils were examined in two transmission electron microscopes, a JEOL TEM 120CX operating at 100 kV and a JEOL TEM 2000FX operating at 200 kV. Chemical analysis of the phases was carried out by X-EDS analysis in the 2000FX using a Be holder to eliminate the possibility of a spurious Cu signal being generated.

During chemical analysis, most of the complicating factors arise because the specimen is not the same as the standard. In the most usual cases a specimen containing several elements is compared with a series of standards, each of which is a pure element. Therefore, the specimen is likely to differ from each standard in its density and in the average atomic weight of its constituent atoms. As a consequence of these differences, some corrections should be made on the specimen concentration. These corrections are for the atomic-number effect, absorption and fluorescence. There are other factors affecting the accuracy of X-ray counting, which are: signal measurements, physical conditions, position of the sample and errors in calibration. Problems can also arise from peak overlaps during chemical analysis. Also, the detector should be stable and as near as possible to the specimen to collect more X-rays. The surface of the specimen should be as flat as possible, otherwise variable geometry will invalidate the correction equations which assume a fixed geometry. Also with very rough surfaces X-rays may be observed by surface protrusion between the area sampled and the detector. In the present work, the accuracy of the thin-foil analysis was within a $\pm 1\%$ range for every element.

X-EDS has certain limitations, such as its resolution limit and the difficulty of analysing low-atomic-number elements. The resolution limit of this technique is due to the interaction volume of the sample with the electron beam and it varies as a function of the atomic number of the element. On average, this volume is about a few micrometres in extent/depth. The analytical point-resolution limits for Cu, Ni, and Cr are roughly equal to 2 μm. Therefore, features finer than this limit could not be analysed. A 220 nm foil thickness was used for all three phases for correct analysis as defined in [6]. The maximum size of the

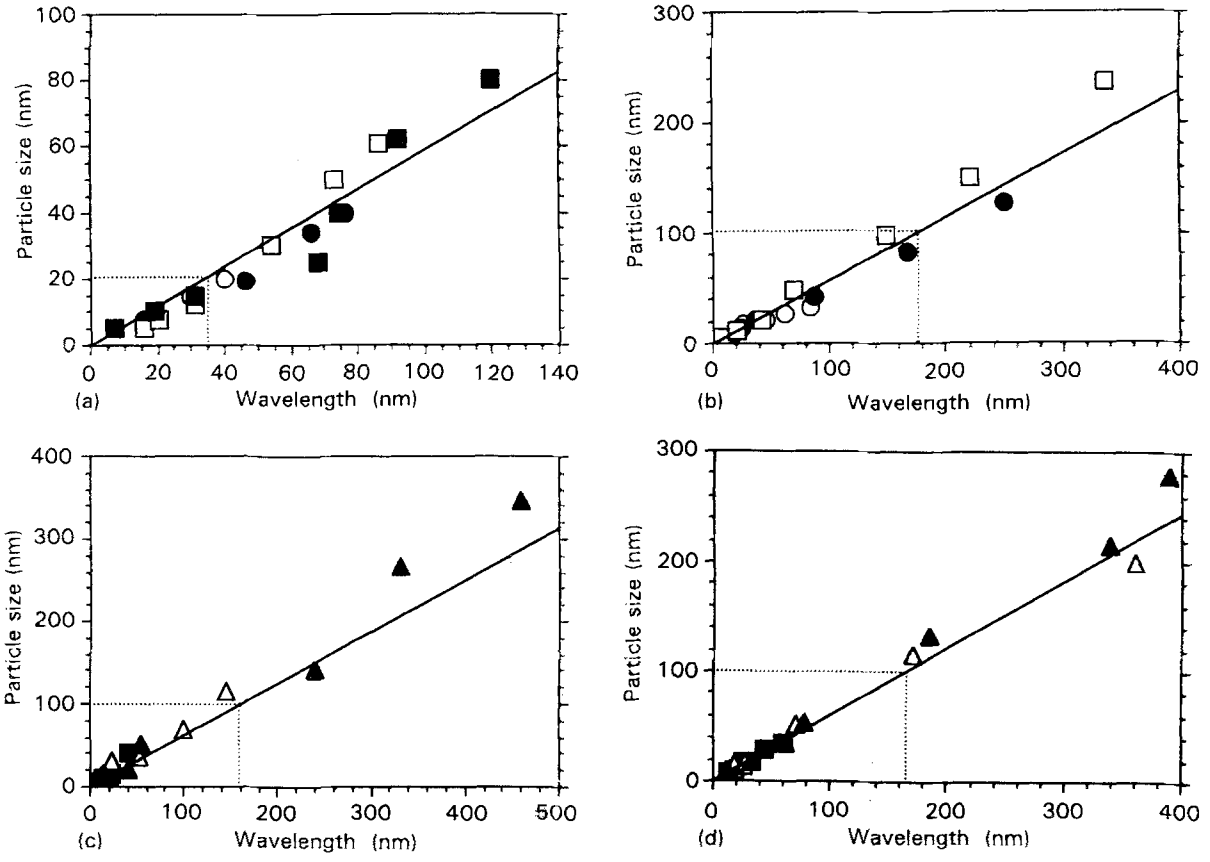

Figure 1 The relationship between particle size and wavelength for different alloys. (a) Cu–30Ni–2.5Cr alloy: (○) 500 °C, (●) 600 °C, (□) 700 °C, and (■) 800 °C. (b) Cu–30Ni–5Cr alloy: (○) 600 °C, (●) 700 °C, and (□) 800 °C. (c) Cu–45Ni–10Cr alloy: (○) 300 °C, (●) 400 °C, (□) 500 °C, (■) 600 °C, (△) 700 °C, and (▲) 800 °C. (d) Cu–45Ni–15Cr alloy: (○) 300 °C, (●) 400 °C, (□) 500 °C, (■) 600 °C, (△) 700 °C, and (▲) 800 °C.

phase particles were 700 nm, 700 nm and 100 nm for Cu-rich, Cu-depleted and Cr-rich phases [6], respectively.

3. Results and discussion

Electron micrographs of the as-quenched samples show some evidence of periodic decomposition products in those alloys. In the early stages of ageing, the characterisitics of spinodal decomposition observed in the XRD and in the electron microscope are [6, 7]: (a) side bands in the XRD, (b) a periodic structure in the electron micrographs of the 15Cr alloy, and (c) constant λ.

In the later stages of decomposition, coarsening of the precipitates takes place in all alloys. The wavelength of decomposition can be measured either directly from the enlarged micrographs (large λ) or by calculation from the spacing of satellite spots in the electron diffraction or from the side bands in the XRD patterns by using the Daniel–Lipson equation [8, 9]. In this work, the wavelength was generally measured from the printed photographs. During the coarsening, both particle size and wavelength increase. For this reason, a direct proportionality may well be expected between particle size and wavelength. In the present study, this particular point was examined and a direct proportionality was obtained. In this relationship, the constant of proportionality increased towards the centre of the miscibility gap. This is consistent with the lever rule. According to this rule, if the alloy lies in the centre of the miscibility gap, a $p = k\lambda$ relationship occurs for an equal amount of phases, then $k = 1$. If the alloy lies away from the central miscibility gap, $k < 1$. The slopes of the curves (Fig. 1) give the relationship between p and λ as $p \sim 0.570\lambda$ for the Cu–30Ni–2.5Cr alloy, $p \sim 0.580\lambda$ for the Cu–30Ni–5Cr alloy, $p \sim 0.628\lambda$ for the Cu–45Ni–10Cr alloy and $p \sim 0.631\lambda$ for the Cu–45Ni–15Cr alloy (e.g. in the 2.5Cr alloy, against a 20 nm particle size, 35 nm wavelength matches through the dashed lines and the p–λ relationship will be $p = (20/35)\lambda$, i.e. $p = 0.570\lambda$ is obtained. Similarly the other p–λ relationships can be found by following this method in the other alloys). These results are in agreement with previous work [10] and confirm that coarsening is taking place without further changes taking place in the phase fraction. It is seen that the particle size/wavelength relationship in the present spinodal alloys is simply $p \propto k\lambda$ and in the symmetrical alloys the proportionality constant k, was greater than in the asymmetrical alloys. A schematic miscibility gap is shown in Fig. 2. Also equal and unequal amounts of phases are illustrated in Figs 3 and 4, respectively.

The asymmetrical alloys have smaller k-values ($k = 0.570$ for the Cu–30Ni–2.5Cr alloy, and $k = 0.580$ for the Cu–30Ni–5Cr alloy) than the symmetrical alloys. This is consistent with the present model. Using these results to calculate the asymmetrical alloys' positions relative to the centre of the miscibility gap, it is seen that the 2.5Cr alloy is 0.43 units ($1 - k = 1 - 0.57 = 0.43$ units) and the 5Cr alloy is 0.42 units ($1 - k = 1 - 0.58 = 0.42$ units) away from the central miscibility gap.

At 930 °C, a ternary diagram is plotted (present result) and compared with those of Meijering *et al.* [4, 5]. Tie lines were determined by X-EDS of both bulk samples, and thin foils. The present ternary diagram at 930 °C (Fig. 5) is in general agreement with that of Meijering *et al.* [4, 5]. However, the corners of the $\alpha + \gamma_1 + \gamma_2$ three-phase area are slightly different from the previous one. The composition of these corners are as follows: γ_1 corner, present result 68Cu–29.3Ni–2.8Cr, Meijering *et al.* 72Cu–27Ni–1Cr; γ_2 corner present result 22.6Cu–55.5Ni–21.9Cr, Meijering *et al.* 24Cu–56Ni–20Cr and α corner, present 1.3Cu–8.5Ni–90.3Cr, Meijering *et al.* 1Cu–11Ni–88Cr. It is observed that in the present results the Cu–Ni–Cr ternary diagram at 930 °C, isothermal section, (Fig. 5) is slightly different from that of Meijering *et al.* [3, 4]. Alloy 2 (5Cr alloy) and alloy 4 (15Cr alloy) lie in the three-phase ($\alpha + \gamma_1 + \gamma_2$) area and in the present study this three-phase area is defined by the three-phase chemical composition of alloy 4. It is clear from Fig. 5 that the volume fraction of the α-phase (Cr-rich) is very small and it is difficult to calculate a ternary diagram with four alloys (Table I). Meijering *et al.* used 35 different alloys to determine the

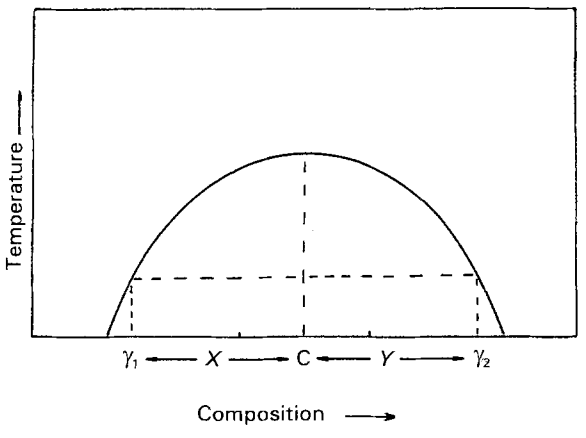

Figure 2 A schematic miscibility gap showing alloy composition versus temperature.

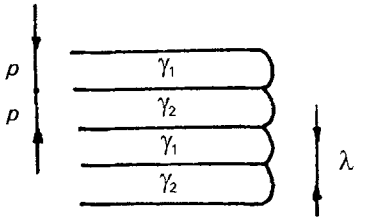

Figure 3 Equal amounts of phases and particle size.

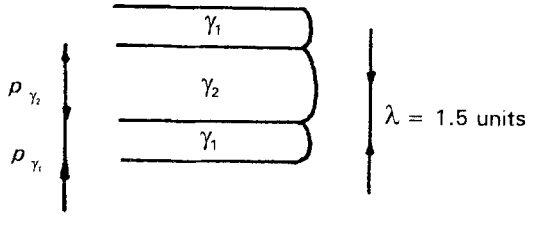

Figure 4 The case $\gamma_1 = 0.5\gamma_2$, and the particle size.

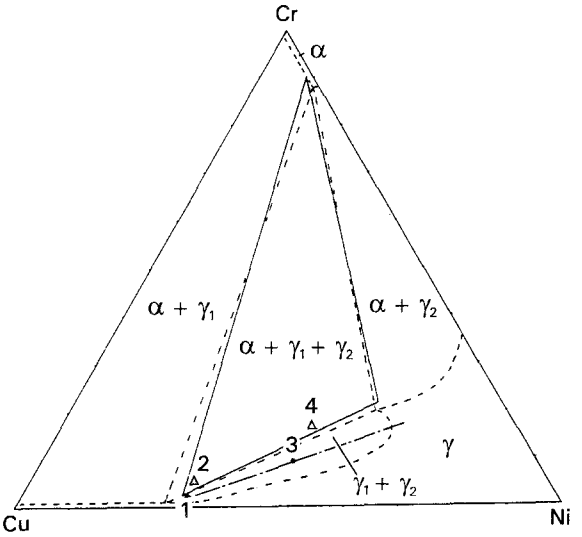

Figure 5 The Cu–Ni–Cr ternary diagram at the 930 °C isothermal section after 3 weeks ageing. (△) shows three phases, (○) shows two phases, (– – –) tie line, (- - -) the results of Meijering *et al.* (——) the results of the present study (wt %).

TABLE I Nominal alloy compositions

Alloy	Cu wt % (at %)	Ni wt % (at %)	Cr wt % (at %)
1	66.4 (64.4)	30.9 (32.4)	2.7 (3.2)
2	66.6 (64.4)	28.5 (29.8)	4.9 (5.8)
3	45.7 (43.1)	44.2 (45.2)	10.1 (11.6)
4	39.7 (37.0)	45.1 (45.6)	15.2 (17.4)

Cu–Ni–Cr ternary system via XRD of bulk specimens. In the present work, using the thin foils for analysis, errors may have been introduced, e.g. some species might be dissolved preferentially or be redeposited. Another reason might be due to electron-microscope-calibration errors or fluorescence effects, because the atomic numbers of Cu, Ni and Cr are close to each other fluorescence effects occur. These possibilities might be reasons for the differences between the present and the previous work [4, 5]. On the other hand, it is not easy and practical to precisely align X-rays. Therefore, it is reasonable to think there are some errors in the XRD results in the previous work [4, 5].

4. Conclusion

Particle size was directly proportional to the wavelength ($p \sim 0.570\lambda$ in a 2.5Cr alloy, $p \sim 0.580\lambda$ in a 5Cr alloy, $p \sim 0.628\lambda$ in a 10Cr alloy and $p \sim 0.631\lambda$ in a 15Cr alloy). Asymmetrical alloys (2.5% and 5%Cr alloys) have smaller k-values than the symmetrical alloys (10% and 15%Cr alloys). All alloys decomposed spinodally, but dilute alloys (2.5–5Cr) lay within the spinodal only at lower temperatures (300–600 °C). The present Cu–Ni–Cr ternary diagram is slightly different from that of Meijering *et al.*, the reason is unclear. It may be possible to clarify this point by preparing more alloys in different regions of the ternary diagram by means of thin-foil and bulk analysis and having the same scientist use transmission electron microscopy and XRD, respectively.

References

1. J. W. GIBBS "The scientific papers" (Dover, New York, 1961) p. 105.
2. P. P. RAO, B. K. AGRAWAL and A. M. RAO, *J. Mater. Sci.* **21** (1986) 3759.
3. *Idem., Trans. Indian Inst. Metals* **26** (1983) 264.
4. J. L. MEIJERING, G. W. RATHENAU, M. G. V. D. STEEG and P. G. BRAUN, *J. Inst. Metals* **84** (1955) 118.
5. J. L. MEIJERING, *Acta Metall.* **5** (1957) 257.
6. F. FINDIK, PhD thesis, Imperial College, London (1992).
7. F. FINDIK and H. M. FLOWER, *Mater. Sci. Technol.* **8** (1992) 197–205.
8. V. DANIEL and H. LIPSON, *Proc. R. Soc. A* **181** (1943) 368.
9. *Idem., ibid. A* **182** (1943) 378.
10. A. J. ARDELL and R. B. NICHOLSON, *ibid.* **22** (1966) 1295.

Received 3 July 1992
and accepted 11 January 1993